

# Quantum treatment of inter-qubit couplers

S. Ashhab,<sup>1</sup> A. O. Niskanen,<sup>2,3</sup> K. Harrabi,<sup>2</sup> Y. Nakamura,<sup>1,2,4</sup> T. Picot,<sup>5</sup>  
P. C. de Groot,<sup>5</sup> C. J. P. M. Harmans,<sup>5</sup> J. E. Mooij,<sup>5</sup> and Franco Nori<sup>1,6</sup>

<sup>1</sup>Frontier Research System, The Institute of Physical and Chemical Research (RIKEN), Wako-shi, Saitama 351-0198, Japan

<sup>2</sup>CREST-JST, Kawaguchi, Saitama 332-0012, Japan

<sup>3</sup>VTT Technical Research Centre of Finland, Sensors, PO BOX 1000, 02044 VTT, Finland

<sup>4</sup>NEC Fundamental Research Laboratories, Tsukuba, Ibaraki 305-8501, Japan

<sup>5</sup>Quantum Transport Group, Kavli Institute of NanoScience,

Delft University of Technology, Lorentzweg 1, 2628 CJ Delft, The Netherlands

<sup>6</sup>Physics Department and Michigan Center for Theoretical Physics,  
The University of Michigan, Ann Arbor, Michigan 48109-1040, USA

(Dated: May 26, 2019)

We consider a system composed of two qubits and a high-excitation-energy quantum object used to mediate coupling between the qubits. We treat the entire system quantum mechanically and analyze the properties of the eigenvalues and eigenstates of the total Hamiltonian. After reproducing well-known results concerning the leading term in the mediated coupling, we obtain an expression for the residual coupling between the qubits in the off state. We also analyze the entanglement between the three objects, i.e. the two qubits and the coupler, in the eigenstates of the total Hamiltonian. Although we focus on the application of our results to the recently realized parametric-coupling scheme with two qubits, we also discuss extensions of our results to a harmonic-oscillator coupler and to multi-qubit systems.

## I. INTRODUCTION

Superconducting qubits are among the main candidates for the possible implementation of quantum-information-processing tasks [1]. Coherent dynamics of a single qubit has been achieved at various laboratories. Several interesting two-qubit experiments have also been performed [2, 3, 4, 5, 6, 7, 8, 9, 10, 11, 12, 13, 14, 15, 16, 17, 18, 19]. The early experiments [2, 3, 4, 5, 6, 7, 8, 9, 10, 11, 12] were limited to fixed inter-qubit coupling. In order to scale up qubit circuits, however, it is highly desirable to be able to tune *in situ* the coupling strengths between the different qubits. The idea of coupling two qubits to a high-excitation-energy quantum object that would mediate coupling between the qubits [20, 21, 22, 23, 24] has led to experimental demonstrations of tunable coupling [13, 14, 15]. However, Refs. [13, 14] probed the low-frequency magnetic susceptibility of the circuit in its ground state; thus the approach used there is not suited to implement the standard gate-based quantum computing, but possibly adiabatic quantum computing [25], where the quantum register is ideally never excited. In Ref. [15] tunability of the coupling was demonstrated through spectroscopic measurements with the qubits biased away from their coherence optimal points. Generalizing the idea of mediated coupling [20, 21, 22, 23, 24] to parametric tunable coupling [26, 27, 28, 29], it was proposed that one can bias the qubits at their coherence optimal points and also adjust the dc component of the mediated coupling to cancel the direct inter-qubit coupling throughout the experiment. Applying a microwave pulse to the coupler at the sum or difference frequency of the qubits' characteristic frequen-

cies would then turn on the coupling, but only for the duration of the applied microwave pulse. This proposal, combining tunable coupling and long coherence times, was realized experimentally in Ref. [17].

Another related direction of growing research activity is the idea of using a harmonic-oscillator 'cavity' as a data bus with the potential that a single cavity could mediate coupling between a large number of qubits [19, 30]. If the harmonic oscillator mediates coupling via high-energy virtual excitations, it can be described similarly to other high-excitation-energy couplers. We shall show, however, that it would be rather difficult to achieve tunability in the coupling in this case.

Early theoretical studies on tunable couplers have generally taken the semiclassical approach, which we shall explain below. The semiclassical treatment is sufficient to evaluate the leading term in the effective coupling mediated by the coupler. As qubit circuits that include couplers are becoming an experimental reality, however, there is an increasing need for a more careful analysis of these quantum couplers. Some recent studies [27, 31, 32] used a number of quantum-mechanical techniques and obtained results beyond the semiclassical calculations (e.g., Ref. [31] derived an expression for the residual coupling term when the main coupling channel is turned off). Here we take a fully quantum approach, where we analyze the properties of the eigenvalues and eigenstates of the total Hamiltonian. We obtain results that were not captured by previous studies, particularly results concerning the ideality of the off state in this coupling scheme.

The main questions of interest that the quantum treatment can be used to answer include: (1) Can we make the coupler's energy splitting very large but still maintain the

mediated coupling between the qubits? (2) Can we turn the coupling off completely? In other words, will there be any residual coupling terms if the system is biased such that the main coupling channel is at its zero point? (3) How much entanglement is there between the qubits and the coupler, and how does this entanglement affect a realistic experimental setup? These questions will be answered in the analysis below.

The paper is organized as follows. In Sec. II we describe the system and its Hamiltonian. In Sec. III we review the semiclassical approach and discuss what predictions we can expect from it regarding the ideality of the off state. In Sec. IV we derive the leading-order effective coupling strength mediated by the coupler, as well as the residual coupling and entanglement between the qubits and the coupler in the off state. We discuss in Sec. V the implications of our results with regard to present-day and future experiments. Section VI contains concluding remarks. Some details of the calculations are explained in the Appendix.

## II. SYSTEM AND HAMILTONIAN

Let us take a system composed of two qubits and a third object that we would like to use as a coupler. Although tunability is considered the main advantage of this coupling scheme, for the purpose of answering the questions of main interest to us it suffices to focus on the case where the external bias parameters are set to fixed values. We therefore treat a time-independent Hamiltonian. Since we are assuming that we can speak of three distinct quantum objects, we must be able to write down a Hamiltonian that reflects this clear separation of the different objects in the system. We therefore express the Hamiltonian as:

$$\hat{H} = \hat{H}_1 + \hat{H}_2 + \hat{H}_C + \hat{H}_{12} + \hat{H}_{1C} + \hat{H}_{2C}, \quad (1)$$

where the first three terms are the Hamiltonians of the separate objects in the system, and the last three terms describe coupling between those objects. As a realistic, representative case, we take the different terms in the Hamiltonian to have the forms:

$$\hat{H}_1 = \frac{\Delta_1}{2} \hat{\sigma}_z^{(1)} + \frac{\epsilon_1}{2} \hat{\sigma}_x^{(1)} \quad (2)$$

$$\hat{H}_2 = \frac{\Delta_2}{2} \hat{\sigma}_z^{(2)} + \frac{\epsilon_2}{2} \hat{\sigma}_x^{(2)} \quad (3)$$

$$\hat{H}_C = \begin{pmatrix} 0 & 0 & 0 & \cdots \\ 0 & \eta_1 & 0 & \\ 0 & 0 & \eta_2 & \\ \vdots & & & \ddots \end{pmatrix} \quad (4)$$

$$\begin{aligned} \hat{H}_{12} &= J_0 \hat{\sigma}_x^{(1)} \otimes \hat{\sigma}_x^{(2)} \\ &= \begin{pmatrix} 0 & 0 & 0 & J_0 \\ 0 & 0 & J_0 & 0 \\ 0 & J_0 & 0 & 0 \\ J_0 & 0 & 0 & 0 \end{pmatrix} \end{aligned} \quad (5)$$

$$\hat{H}_{1C} = \hat{\sigma}_x^{(1)} \otimes \hat{A} \quad (6)$$

$$\hat{H}_{2C} = \hat{\sigma}_x^{(2)} \otimes \hat{B}, \quad (7)$$

with the coupler energies  $0, \eta_1, \eta_2, \dots$  arranged in increasing order,

$$\hat{A} = \begin{pmatrix} A_{00} & A_{01} & A_{02} & \cdots \\ A_{10} & A_{11} & A_{12} & \\ A_{20} & A_{21} & A_{22} & \\ \vdots & & & \ddots \end{pmatrix}, \quad (8)$$

and similarly for  $\hat{B}$ . For the case of superconducting flux qubits,  $\Delta_j$  is the minimum gap of qubit  $j$ ,  $\epsilon_j$  represents the deviation from the degeneracy point of half-integer flux quantum threading the qubit loop [i.e.  $\epsilon_j = I_{p,j}(\Phi_{\text{ext},j} - \Phi_0/2)$ , where  $I_{p,j}$  is the persistent current of qubit  $j$ ,  $\Phi_{\text{ext},j}$  is the externally applied flux in the loop of qubit  $j$ , and  $\Phi_0$  is the flux quantum],  $J_0$  is the direct qubit-qubit coupling strength, and  $\hat{\sigma}_\alpha^{(j)}$  are the usual Pauli matrices of qubit  $j$ . Note that the minimum gap  $\Delta_j$  is the coefficient of  $\hat{\sigma}_z^{(j)}$  above, in contrast with some alternative conventions used in the literature where  $\Delta_j$  is the coefficient of  $\hat{\sigma}_x^{(j)}$ . Note also that the operators  $\hat{A}$  and  $\hat{B}$  must satisfy  $A_{ij} = A_{ji}^*$  and  $B_{ij} = B_{ji}^*$ . The coupler's Hamiltonian  $\hat{H}_C$  is written in its own eigenbasis (thus it is diagonal), and its ground-state energy has been set to zero. We shall express Hamiltonians and energies in frequency units throughout this paper.

We now make the assumption that the largest energy scale in the problem is the excitation energy of the coupler. In other words  $\eta_1$  is larger than any relevant energy scale in the Hamiltonian excluding  $\hat{H}_C$ . We shall not make any assumption regarding the relation between the qubit energy scale  $\sqrt{\Delta_j^2 + \epsilon_j^2}$  and the qubit-coupler coupling energy scale (i.e. the scale of the matrix elements in  $\hat{A}$  and  $\hat{B}$ ). Although it is not crucial for most of our analysis below, we shall generally take the direct coupling energy scale  $J_0$  to be smaller than the qubit energy scale.

## III. SEMICLASSICAL TREATMENT

Before embarking on the semiclassical description of our system, it is instructive to recall the problem of calculating interatomic forces within the hydrogen molecule [33]. One starts by assuming that the nuclei have fixed locations in space, leaving the degrees of freedom associated with electron motion as the only variables in the problem. The ground state of the electronic degrees of freedom is calculated and expressed as a function of the distance between the nuclei. At this point, the total energy (direct Coulomb energy of the nuclei plus electronic ground-state energy) is expressed as a function of the relative position operator between the nuclei, and the nuclear motion is treated quantum mechanically. One can now obtain information related to atomic motion

or molecular eigenstates without having to worry about electronic motion. The first step of the calculation ensures that the effects of the electrons' adiabatic adjustment to nuclear motion are properly taken into account. The reason why the electronic degrees of freedom can adjust adiabatically to nuclear motion is that they are associated with a much higher energy scale, and thus changes that result from nuclear motion are felt by the electrons as very slow variations.

A similar procedure can be applied when dealing with inter-qubit couplers. Since the qubit-coupler interactions contain the operators  $\hat{\sigma}_x^{(j)}$ , one first assumes that the qubits are in eigenstates of  $\hat{\sigma}_x^{(j)}$ . One therefore needs to calculate the ground state energy of the Hamiltonian (or, more precisely, the four Hamiltonians):

$$\begin{aligned} \hat{H}_{C,\text{eff}} &\equiv \hat{H}_C + \hat{H}_{1C} + \hat{H}_{2C} \\ &\xrightarrow{\sigma_x^{(j)}=\pm 1} \hat{H}_C \pm \hat{A} \pm \hat{B}. \end{aligned} \quad (9)$$

The ground state energy [i.e. the four values obtained from Eq. (9)] can then be expressed in the form:

$$\text{Gnd state energy } \left\{ \hat{H}_{C,\text{eff}} \right\} = c_1 + c_2 \sigma_x^{(1)} + c_3 \sigma_x^{(2)} + c_4 \sigma_x^{(1)} \otimes \sigma_x^{(2)} \quad (10)$$

Note that we have started with the assumption that the qubits have well-defined values of  $\sigma_x^{(j)}$ . One could therefore say that the above expression is not a quantum operator. However, it is straightforward to follow the adiabaticity argument: the coupler will, to a very good approximation, always be in the ground state that corresponds to the instantaneous values of  $\sigma_x^{(j)}$  (including the possibility of quantum superpositions). One can therefore turn back to the qubits and analyze their dynamics using the effective Hamiltonian:

$$\hat{H}_{q,\text{eff}} = \hat{H}_1 + \hat{H}_2 + \hat{H}_{12} + \hat{H}_{\text{mediated}}, \quad (11)$$

where

$$\hat{H}_{\text{mediated}} = c_1 + c_2 \hat{\sigma}_x^{(1)} + c_3 \hat{\sigma}_x^{(2)} + c_4 \hat{\sigma}_x^{(1)} \otimes \hat{\sigma}_x^{(2)}. \quad (12)$$

The above derivation shows that the response of the coupler to external perturbations (induced by the qubits and represented by the terms  $\pm \hat{A}$  and  $\pm \hat{B}$ ) translates into a renormalization of the qubit bias points [second and third term in Eq. (12)] and an additional coupling term between the qubits [last term in Eq. (12)].

It is interesting to note here that in the semiclassical treatment above, the effect of the coupler on the qubits is completely described by the Hamiltonian  $\hat{H}_{\text{mediated}}$ . Therefore, if the bias point is chosen such that the coefficient  $c_4$  in Eq. (12) cancels the direct coupling strength  $J_0$ , there would be no residual coupling between the qubits. The off state would therefore correspond to complete decoupling between the qubits. In contrast, we shall show below that the fully quantum treatment predicts the presence of finite residual coupling effects.

#### IV. QUANTUM TREATMENT

We now take the Hamiltonian of Sec. II (Eq. 1) and treat it quantum mechanically. In particular, we would like to analyze the properties of the eigenvalues and eigenstates of the total Hamiltonian. For the purposes of the calculations in this section, we divide the Hamiltonian into two parts as follows:

$$\hat{H} = \hat{H}_0 + \hat{V}, \quad (13)$$

where

$$\hat{H}_0 = \frac{\Delta_1}{2} \hat{\sigma}_z^{(1)} + \frac{\Delta_2}{2} \hat{\sigma}_z^{(2)} + \hat{H}_C \quad (14)$$

$$\hat{V} = \frac{\epsilon_1}{2} \hat{\sigma}_x^{(1)} + \frac{\epsilon_2}{2} \hat{\sigma}_x^{(2)} + \hat{H}_{12} + \hat{H}_{1C} + \hat{H}_{2C}. \quad (15)$$

We use the basis  $\{|000\rangle, |010\rangle, |100\rangle, |110\rangle, |001\rangle, |011\rangle, |101\rangle, |111\rangle, |002\rangle, \dots\}$ , where the first, second and third quantum numbers describe, respectively, the state of the first qubit, second qubit and coupler (the state of the coupler will be distinguished from those of the qubits using an underline throughout this paper); note that we allow the coupler to have more than two levels. We can now express  $\hat{H}_0$  as

$$\hat{H}_0 = \begin{pmatrix} \frac{-\Delta_1 - \Delta_2}{2} & 0 & 0 & 0 & & & & & \dots \\ 0 & \frac{-\Delta_1 + \Delta_2}{2} & 0 & 0 & & & & & \\ 0 & 0 & \frac{\Delta_1 - \Delta_2}{2} & 0 & & & & & \\ 0 & 0 & 0 & \frac{\Delta_1 + \Delta_2}{2} & & & & & \\ & & & & \eta_1 + \frac{-\Delta_1 - \Delta_2}{2} & 0 & 0 & 0 & \\ & & & & 0 & \eta_1 + \frac{-\Delta_1 + \Delta_2}{2} & 0 & 0 & \\ & & & & 0 & 0 & \eta_1 + \frac{\Delta_1 - \Delta_2}{2} & 0 & \\ & & & & 0 & 0 & 0 & \eta_1 + \frac{\Delta_1 + \Delta_2}{2} & \\ \vdots & & & & & & & & \ddots \end{pmatrix}. \quad (16)$$

As we shall see shortly, this separation of terms will allow us to find good approximations for the eigenstates and

their energies.

### A. Coupling strength: leading term

In order to calculate the effective coupling strength, we now calculate the energies of the lowest four energy levels. We therefore want to construct a  $4 \times 4$  effective-Hamiltonian matrix describing the lowest energy levels while taking into account the effects of the higher levels.

We now follow a standard calculation [34] (see Appendix) that gives:

$$\hat{H}_{\text{eff}} \approx \hat{H}_{\text{eff}}^{(0)} + \hat{H}_{\text{eff}}^{(1)} + \hat{H}_{\text{eff}}^{(2)} \quad (17)$$

where

$$\hat{H}_{\text{eff}}^{(0)} = \hat{H}_1 + \hat{H}_2 + \hat{H}_{12} = \frac{1}{2} \begin{pmatrix} -\Delta_1 - \Delta_2 & \epsilon_2 & \epsilon_1 & 2J_0 \\ \epsilon_2 & -\Delta_1 + \Delta_2 & 2J_0 & \epsilon_1 \\ \epsilon_1 & 2J_0 & \Delta_1 - \Delta_2 & \epsilon_2 \\ 2J_0 & \epsilon_1 & \epsilon_2 & \Delta_1 + \Delta_2 \end{pmatrix} \quad (18)$$

$$\hat{H}_{\text{eff}}^{(1)} = A_{00}\sigma_x^{(1)} + B_{00}\sigma_x^{(2)} = \begin{pmatrix} 0 & B_{00} & A_{00} & 0 \\ B_{00} & 0 & 0 & A_{00} \\ A_{00} & 0 & 0 & B_{00} \\ 0 & A_{00} & B_{00} & 0 \end{pmatrix} \quad (19)$$

$$\hat{H}_{\text{eff}}^{(2)} = \sum_{l=1}^{\infty} \sum_{k=00,01,10,11} \hat{P} \frac{\hat{V}|k,l\rangle\langle k,l|\hat{V}}{\hat{H}_{\text{eff}} - E_{k,l}} \hat{P}, \quad (20)$$

where the operator  $\hat{P}$  projects the state onto the space of the lowest four eigenstates of  $H_0$  ( $|000\rangle$ ,  $|010\rangle$ ,  $|100\rangle$  and  $|110\rangle$ ); alternatively, one could say that the operator  $\hat{P}$  removes the size mismatch between the four-dimensional quantum states and the infinite-dimensional operator  $\hat{V}$ . The sum over  $l$  in Eq. (20) runs over states where the coupler is in one of its excited states. To lowest order Eq. (20) gives

$$\begin{aligned} \hat{H}_{\text{eff}}^{(2)} &= \hat{H}_{\text{coupling}}^{(2)} + \hat{H}_{\text{shift}}^{(2)} \quad (21) \\ \hat{H}_{\text{coupling}}^{(2)} &\approx \begin{pmatrix} 0 & 0 & 0 & -J_1 \\ 0 & 0 & -J_1 & 0 \\ 0 & -J_1 & 0 & 0 \\ -J_1 & 0 & 0 & 0 \end{pmatrix} = -J_1 \hat{\sigma}_x^{(1)} \otimes \hat{\sigma}_x^{(2)} \\ \hat{H}_{\text{shift}}^{(2)} &\approx -\Delta_{\text{shift}} \begin{pmatrix} 1 & 0 & 0 & 0 \\ 0 & 1 & 0 & 0 \\ 0 & 0 & 1 & 0 \\ 0 & 0 & 0 & 1 \end{pmatrix} \end{aligned}$$

where

$$\begin{aligned} J_1 &= \sum_{l=1}^{\infty} \frac{A_{0l}B_{l0} + B_{0l}A_{l0}}{\eta_l} \\ \Delta_{\text{shift}} &= \sum_{l=1}^{\infty} \frac{|A_{0l}|^2 + |B_{0l}|^2}{\eta_l}. \quad (22) \end{aligned}$$

The overall shift  $\hat{H}_{\text{shift}}^{(2)}$  does not have any physical con-

sequences to this order of the calculation and can be neglected.

The effective Hamiltonian can now be expressed as

$$\hat{H}_{\text{eff}} = \tilde{H}_0 + \tilde{H}_{\text{coupling}}, \quad (23)$$

where

$$\begin{aligned} \tilde{H}_0 &= \frac{\Delta_1}{2} \hat{\sigma}_z^{(1)} + \frac{\tilde{\epsilon}_1}{2} \hat{\sigma}_x^{(1)} + \frac{\Delta_2}{2} \hat{\sigma}_z^{(2)} + \frac{\tilde{\epsilon}_1}{2} \hat{\sigma}_x^{(2)} \\ \tilde{H}_{\text{coupling}} &= J \hat{\sigma}_x^{(1)} \otimes \hat{\sigma}_x^{(2)}, \end{aligned}$$

with the parameters

$$\begin{aligned} \tilde{\epsilon}_1 &= \epsilon_1 + 2A_{00} \\ \tilde{\epsilon}_2 &= \epsilon_2 + 2B_{00} \\ J &= J_0 - J_1. \quad (24) \end{aligned}$$

The above results agree with those of Ref. [27] when the parameters of our model are taken to correspond to those considered in Ref. [27].

In order to clarify some of the above results, we give their interpretation in the experimentally relevant case of flux qubits. In order to bias the qubits at their optimal points, the externally applied fluxes through the qubit loops are not set to  $\Phi_0/2$ , but they are shifted from that value to compensate for the fluxes generated by the coupler (in its ground state) and going through the qubit loops. This is the physical explanation of the difference

between  $\epsilon_j$  and  $\tilde{\epsilon}_j$  [35]. Assuming that the three externally applied fluxes through the three loops in the circuit can be adjusted independently, we can now bias the coupler at the desired working point for coupling purposes, e.g. to set  $J = 0$ , and eliminate  $\tilde{\epsilon}_1$  and  $\tilde{\epsilon}_2$ , i.e. three tunable parameters used to satisfy three requirements.

We can now answer the question of how high the coupler's energy splitting can be. We note that the mediated coupling strength  $J_1$  is second order in the scale of  $\hat{A}$  and  $\hat{B}$ , and it is inversely proportional to the scale of  $\eta_l$ . Although this means that we cannot simply take  $\eta_l \rightarrow \infty$  keeping the other parameters fixed (otherwise  $J_1 \rightarrow 0$ ), it also means that if we increase  $A_{nm}$ ,  $B_{nm}$  and  $\eta_l$  (keeping the ratio  $A_{0l}B_{l0}/\eta_l$  fixed) we can in fact take  $\eta_l \rightarrow \infty$  while maintaining the same level of mediated coupling. We shall see below that this situation is desirable for purposes of reducing residual-coupling effects.

We are also in a position to comment on the question of monostability of the coupler (i.e. the idea that a single energy level of the coupler is relevant in the system under consideration). The presence of the matrix elements  $A_{l0}$  and  $B_{l0}$ , which describe coupling between the coupler's ground and excited states, in the expression for the mediated coupling strength (Eq. 22) demonstrates that the excited states of the coupler play an important role in the coupling mechanism. The semiclassical treatment relies on the fact that the relevant information contained in these matrix elements is also included, and more easily accessible experimentally, in the response of the coupler's ground state to weak perturbations. As a result, knowledge of the matrix elements themselves is not necessary; knowledge of simple response parameters is sufficient in order to calculate the mediated coupling strength.

### B. Residual coupling in the off state

In order to calculate higher-order corrections in the quantum description, we follow the philosophy of degenerate perturbation theory: once we treat the lowest order carefully and find the suitable basis where the degeneracy is lifted, we can use that basis and proceed in a systematic manner to obtain higher-order corrections, possibly to all orders.

Since we are interested in an ideal off state with the qubits at their optimal points, we take  $J = \tilde{\epsilon}_1 = \tilde{\epsilon}_2 = 0$ . In order to enhance the robustness of the decoupling between the qubits, we impose the additional requirement that  $\Delta_1 \neq \Delta_2$ . The effective Hamiltonian (Eq. 23) is diagonal to lowest order in this case. We can therefore start the perturbative calculation from the states  $|000\rangle$ ,  $|010\rangle$ ,  $|100\rangle$  and  $|110\rangle$ .

As will be discussed in Sec. V, one of the most relevant calculations in this context is that of the energies of the lowest four levels of the entire system (we shall refer to them as  $E_{000}$ ,  $E_{010}$ ,  $E_{100}$ , and  $E_{110}$ ). The four values that we obtain for the energies in the four-level spectrum can then be used to extract four quantities: (1) an overall

energy that can be neglected, (2,3) the corrected (i.e. renormalized) values of the qubit splittings  $\Delta_j$  and (4) a residual-coupling energy (given by  $E_{000} + E_{110} - E_{010} - E_{100}$ ) that characterizes an interaction term of the form  $\hat{\sigma}_z^{(1)} \otimes \hat{\sigma}_z^{(2)}$  [36]. It is this last quantity that is of most interest to us here. It results in a coupling Hamiltonian of the form:

$$\hat{H}_{\text{residual}} = J_{\text{residual}} \hat{\sigma}_z^{(1)} \otimes \hat{\sigma}_z^{(2)}, \quad (25)$$

where

$$J_{\text{residual}} = \frac{E_{000} + E_{110} - E_{010} - E_{100}}{4}. \quad (26)$$

Although one can make analytic progress calculating the energies using the pseudo-degenerate perturbation theory approach, reaching the relevant results requires several steps of the iterative procedure explained in the Appendix (the lowest-order corrections to the individual energies do not contribute to the combination  $E_{000} + E_{110} - E_{010} - E_{100}$ ). We therefore only present the results of numerical calculations that find the energy levels of the entire system. It also turns out that proceeding with the rather general model used so far complicates the extraction of the important results. We therefore have to make some simplifying assumptions. From now on, we restrict ourselves to a simple case that also happens to be relevant to recent experiments: we take the coupler to be a two-level system, such that

$$\begin{aligned} \hat{H}_C &= \frac{\epsilon_C}{2} \hat{\sigma}_x^{(C)} + \frac{\Delta_C}{2} \hat{\sigma}_z^{(C)} \\ &= \frac{\Delta_C}{2} \left( \tan \theta_C \hat{\sigma}_x^{(C)} + \hat{\sigma}_z^{(C)} \right) \\ \hat{H}_{1C} &= J_{1C} \hat{\sigma}_x^{(1)} \otimes \sigma_x^{(C)} \\ \hat{H}_{2C} &= J_{2C} \hat{\sigma}_x^{(2)} \otimes \sigma_x^{(C)} \end{aligned} \quad (27)$$

(note that, unlike the convention used in Sec. II,  $\hat{H}_C$  is not diagonal here). We therefore have  $\eta_1 = \sqrt{\Delta_C^2 + \epsilon_C^2} = \Delta_C / |\cos \theta_C|$ ,  $A_{00} = -A_{11} = -J_{1C} \sin \theta_C$ ,  $A_{10} = A_{01} = J_{1C} \cos \theta_C$  and similarly for  $\hat{B}$ . As a result, we find from Eq. (22) that

$$J = J_0 - \frac{2J_{1C}J_{2C} \cos^3 \theta_C}{\Delta_C}. \quad (28)$$

We consider the parametric-coupling scheme [26, 27, 28], and we start by noting three factors that can contribute to determining the ideal dc bias point. Firstly, we note from Eq. (28) that the effective coupling strength  $J$  ranges from  $J_0 - 2J_{1C}J_{2C}/\Delta_C$  (at  $\theta_C = 0$ ) to  $J_0$  (at  $\theta_C = \pi/2$ ). In order to maximize the effective coupling strength of the parametric-coupling scheme, it would be desirable to set the dc bias point such that  $J = J_0 - J_{1C}J_{2C}/\Delta_C$ , i.e. halfway between the two extremes; This situation is obtained by setting  $\theta_C \approx 0.65 \approx \pi/5$ . At this bias point, the allowed amplitude of the ac driving signal (i.e. before encountering nonlinearities in  $J$ ) is

maximized (see Fig. 1a). Secondly, it is desirable to set  $J = 0$  at the dc bias point. Thirdly, it is also desirable to set the residual coupling energy  $J_{\text{residual}} = 0$ .

We start by taking the first two conditions above, and we proceed as follows: We first fix the parameters  $\Delta_1$ ,  $\Delta_2$ ,  $\Delta_C$  and  $J_0$  (e.g.  $\Delta_1 = 4$  GHz,  $\Delta_2 = 5$  GHz,  $\Delta_C = 30$  GHz and  $J_0 = 50$  MHz). The coupling strengths  $J_{1C}$  and  $J_{2C}$  are now chosen as  $J_{1C} = J_{2C}$  and  $J_{1C}J_{2C}/\Delta_C = J_0$ . The above choice ensures that the same dc bias point satisfies both conditions (i.e.  $J$  vanishes while maximizing the achievable effective coupling strength for the parametric-coupling scheme). The coupler's bias point,

$$J_{\text{residual}} \approx 4 \frac{\Delta_1 \Delta_2 J_0 J_{1C} J_{2C}}{\Delta_C^4} \cos^6 \theta_C - \alpha \frac{\Delta_1 \Delta_2 J_{1C}^2 J_{2C}^2}{\Delta_C^5} \cos^5 \theta_C \sin^2(2\theta_C), \quad (29)$$

where the coefficient  $\alpha$  is approximately 20.

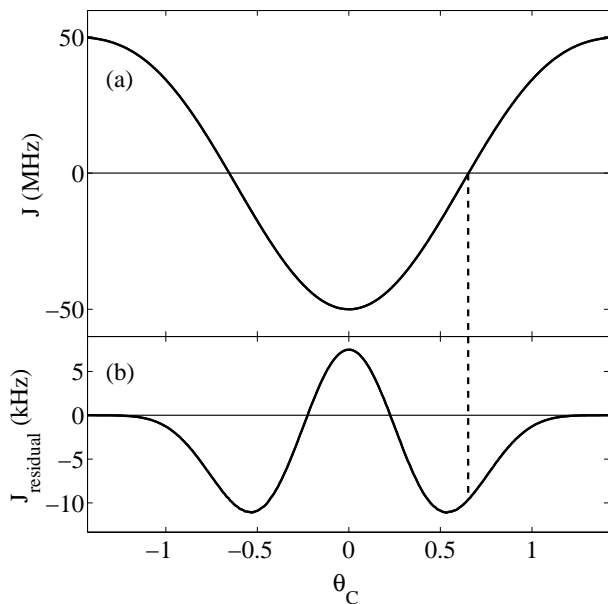


FIG. 1: Coefficients of the main (a) and residual (b) coupling terms (i.e.  $J$  and  $J_{\text{residual}}$ ) as functions of the coupler's bias point  $\theta_C$ . In generating this figure we took  $\Delta_1 = 4$  GHz,  $\Delta_2 = 5$  GHz,  $\Delta_C = 30$  GHz,  $J_0 = 50$  MHz and  $J_{1C} = J_{2C} = \sqrt{J_0 \Delta_C}$ . It should be noted, however, that the results are only weakly dependent on the exact choice of parameters.

It is encouraging for future experimental efforts that the residual-coupling term obtained above decreases rapidly with increasing coupler gap  $\Delta_C$ , even if the mediated coupling strength is kept at a fixed level. Furthermore, it is possible to adjust the system parameters such that the conditions of vanishing  $J$  and  $J_{\text{residual}}$  are simultaneously satisfied. An example of this situation is shown in Fig. 2. Note that the achievable effective cou-

pling strength for the parametric-coupling scheme has been reduced from that in Fig. 1, because the dc bias point is now close to  $\theta_C = 0$  (or  $\epsilon_C = 0$ ), one endpoint in the range of  $J$  values.

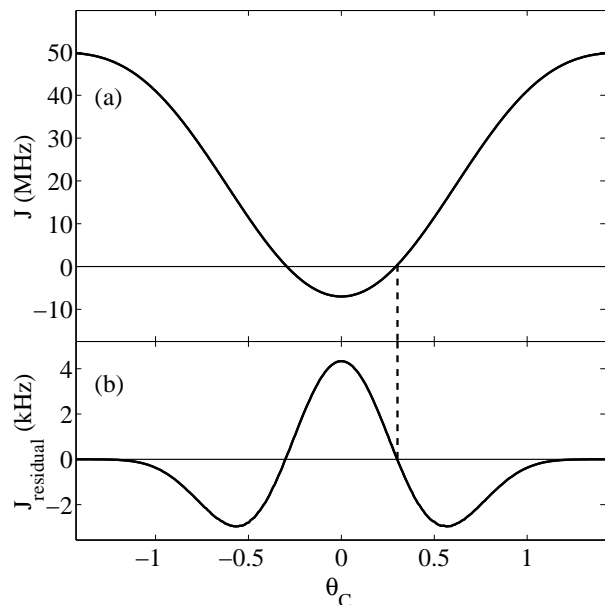


FIG. 2: Same as in Fig. 1, except that  $J_{1C} = J_{2C} = 0.75\sqrt{J_0 \Delta_C}$ . As opposed to Fig. 1,  $J$  and  $J_{\text{residual}}$  now vanish at the same bias point.

pling strength for the parametric-coupling scheme has been reduced from that in Fig. 1, because the dc bias point is now close to  $\theta_C = 0$  (or  $\epsilon_C = 0$ ), one endpoint in the range of  $J$  values.

### C. Entanglement in the eigenstates

The next natural question to ask is the amount of entanglement between the qubits and the coupler, and between the qubits themselves, in the different eigenstates. Here we are interested in the nearly ideal situation where

any residual entanglement is treated as a small error. We therefore take the situation analyzed in the previous subsection ( $J = \tilde{\epsilon}_1 = \tilde{\epsilon}_2 = 0$ ,  $\Delta_1 \neq \Delta_2$ , and the coupler is a two-level system), and we analyze the degree of entanglement to lowest non-vanishing orders.

As explained earlier in this section, we can start our calculation from the states  $|000\rangle$ ,  $|010\rangle$ ,  $|100\rangle$  and  $|110\rangle$ . For the lowest order of this calculation, we can use the pseudo-degenerate perturbation theory calculation explained in the Appendix. We find that

$$|\psi_{00}\rangle \approx |000\rangle - \frac{J_0}{2\eta_1}|110\rangle - \frac{A_{10}}{\eta_1}|101\rangle - \frac{B_{10}}{\eta_1}|011\rangle$$

$$\begin{aligned} |\psi_{01}\rangle &\approx |010\rangle - \frac{J_0}{2\eta_1}|100\rangle - \frac{A_{10}}{\eta_1}|111\rangle - \frac{B_{10}}{\eta_1}|001\rangle \\ |\psi_{10}\rangle &\approx |100\rangle - \frac{J_0}{2\eta_1}|010\rangle - \frac{A_{10}}{\eta_1}|001\rangle - \frac{B_{10}}{\eta_1}|111\rangle \\ |\psi_{11}\rangle &\approx |110\rangle - \frac{J_0}{2\eta_1}|000\rangle - \frac{A_{10}}{\eta_1}|011\rangle - \frac{B_{10}}{\eta_1}|101\rangle \end{aligned} \quad (30)$$

up to a normalization constant slightly smaller than 1. Note that the above expressions can collectively be summarized as [37]:

$$\begin{aligned} |\psi_{nm}\rangle &\approx |nm0\rangle - \frac{J_0}{2\eta_1}|\bar{n}\bar{m}0\rangle - \frac{A_{10}}{\eta_1}|\bar{n}m1\rangle - \frac{B_{10}}{\eta_1}|n\bar{m}1\rangle \\ &= \left(1 - \frac{J_0}{2\eta_1}\hat{\sigma}_x^{(1)} \otimes \hat{\sigma}_x^{(2)} - \frac{A_{10}}{\eta_1}\hat{\sigma}_x^{(1)} \otimes \hat{\sigma}_x^{(C)} - \frac{B_{10}}{\eta_1}\hat{\sigma}_x^{(2)} \otimes \hat{\sigma}_x^{(C)}\right)|nm0\rangle \\ &= \left(1 - \frac{J_0 \cos \theta_C}{2\Delta_C}\hat{\sigma}_x^{(1)} \otimes \hat{\sigma}_x^{(2)} - \frac{J_{1C} \cos^2 \theta_C}{\Delta_C}\hat{\sigma}_x^{(1)} \otimes \hat{\sigma}_x^{(C)} - \frac{J_{2C} \cos^2 \theta_C}{\Delta_C}\hat{\sigma}_x^{(2)} \otimes \hat{\sigma}_x^{(C)}\right)|nm0\rangle. \end{aligned} \quad (31)$$

Two notes are in order here: (1) The mixing of computational-basis states in the eigenstates (Eq. 31) cannot be identified as arising from a simple residual-coupling Hamiltonian. This can be perhaps most clearly seen in the fact that the signs in front of the small terms in Eq. (31) are independent of the state. In contrast, one always expects different states to acquire corrections of different signs when dealing with a direct coupling Hamiltonian. Higher-order effects in this system therefore cannot be completely described by simply using small corrections to the reduced (i.e.  $4 \times 4$ ) two-qubit Hamiltonian. (2) The above expressions were obtained assuming only that the coupling strength  $J$  vanishes and  $\Delta_1 \neq \Delta_2$ . They are not affected by the value of the residual-coupling Hamiltonian discussed in Sec. IV.B. This fact demonstrates that the vanishing of both  $J$  and  $J_{\text{residual}}$  does not imply that the qubits are entirely decoupled. Corrections to the eigenstates still have to be considered when calculating possible errors.

As in the case of the residual-coupling Hamiltonian, it is encouraging for scalability considerations that the entanglement in the eigenstates decreases and approaches zero with increasing  $\Delta_C$ , assuming that  $J_0$  and  $J_1$  are kept fixed. One can therefore say that the coupler becomes more and more ideal as  $\Delta_C$  is increased. It should be noted that, with present-day designs of flux qubits, it would be difficult to make  $\Delta_C$  larger than  $\sim 50$  GHz.

#### D. Harmonic oscillator as a coupler

We can use the results derived above for a two-level coupler to infer the corresponding results for a harmonic-oscillator coupler. We now consider the situation where

$$\begin{aligned} \hat{H}_C &= \omega_C \hat{a}^\dagger \hat{a} \\ \hat{H}_{1C} &= J_{1C} \hat{\sigma}_x^{(1)} \otimes (\hat{a} + \hat{a}^\dagger) \\ \hat{H}_{2C} &= J_{2C} \hat{\sigma}_x^{(2)} \otimes (\hat{a} + \hat{a}^\dagger), \end{aligned} \quad (32)$$

where  $\hat{a}^\dagger$  and  $\hat{a}$  are the creation and annihilation operators for the coupler. The above coupling Hamiltonians change the state of the coupler by one excitation. It should therefore be a good approximation to truncate the coupler to its lowest two energy levels. We now find that

$$J = J_0 - \frac{2J_{1C}J_{2C}}{\omega_C} \quad (33)$$

and

$$J_{\text{residual}} \approx 4 \frac{\Delta_1 \Delta_2 J_0 J_{1C} J_{2C}}{\omega_C^4}. \quad (34)$$

In order to study the tunability of a harmonic-oscillator coupler, we now consider the effect of an applied external field on the mediated coupling, adding the term

$$\hat{H}_{\text{field}} = E (\hat{a} + \hat{a}^\dagger) \quad (35)$$

to the Hamiltonian. By defining  $\hat{b} \equiv \hat{a} + 2E/\omega_C$ , we can see that the new Hamiltonian takes the same form it had

in the absence of  $\hat{H}_{\text{field}}$ , except that  $\hat{a}$  and  $\hat{a}^\dagger$  are replaced by  $\hat{b}$  and  $\hat{b}^\dagger$ , and the qubit bias parameters  $\epsilon_1$  and  $\epsilon_2$  are shifted to  $\tilde{\epsilon}_1$  and  $\tilde{\epsilon}_2$  (just as discussed in the general case above). In particular, the values of  $J$  and  $J_{\text{residual}}$  are not affected by the applied field. The mediated coupling is therefore not tunable, assuming that the coupler's bias point is set by an applied linear field, i.e. a field that affects the coupler according to Eq. (35).

If the frequency of the harmonic oscillator (or alternatively  $J_{1C}$  and  $J_{2C}$ ) were tunable, one would be able to obtain a tunable value of  $J$  (see Eq. 33). Possible designs for such tunable couplers have been proposed theoretically [38], but they have not been realized experimentally. Given the advantages they could provide in terms of tunable coupling, it would be highly desirable to fabricate such tunable oscillators in the future. We should mention here that setting  $J = 0$  in the off state, which is the main advantage of the tunable coupling approach, is much better suited for scalable circuits than the approach of effectively decoupling the qubits by simply setting  $|J| \ll |\Delta_1 - \Delta_2|$  [39]. This point will be discussed further in Sec. V.B below.

A related design would be to use a large (possibly non-tunable) harmonic-oscillator element in the circuit and add a tunable coupler between this oscillator and each qubit around it. With this design one would gain the advantages of both (1) the large ‘cavity’ being able to function as a data bus connecting a large number of qubits and (2) the coupling being tunable. With this design one would also be able to use the parametric-coupling scheme to perform entangling operations on any qubit in the circuit and the cavity relatively easily (using red- or blue-sideband transitions), with the qubits biased at their optimal points.

## V. ESTIMATING ERRORS IN A TYPICAL EXPERIMENT

In this section we discuss a typical present-day experimental procedure. Using concrete examples, we will be able to discuss rather clearly the possible errors that the residual coupling and eigenstate entanglement might cause.

In most, if not all, present-day experiments, the qubits are controlled using a single microwave line. This situation, however, cannot be maintained for larger multi-qubit systems, where the energy levels of the entire system become densely packed. We shall therefore assume that local control lines are used to address the individual qubits.

### A. Two-qubit system

The usual theoretical approach to describing a quantum system that is composed of several distinct objects commonly runs along the following line of reasoning: first

we assume that these objects are in a separable initial state, then we controllably evolve the system using the total Hamiltonian, we take the trace over the degrees of freedom of the unused objects (in this case the coupler), and we find the answer to the physical questions of interest. Given the entangled form of the eigenstates obtained in Sec. IV, one might expect that this ‘contamination’ of the states will reduce the observed coherence effects. Indeed, following the above-described recipe, one finds such a reduction in observable coherence effects, e.g. reduced gate fidelities. As we now explain, however, this is not the correct description of a typical experiment, and the resulting errors and limitations are also described incorrectly in this way.

First let us consider the assumption about the initial conditions. In a real two-qubit experiment (assuming essentially zero temperature), the system starts in its ground state  $|\psi_{00}\rangle \neq |00\rangle$ . When preparing the desired initial state (e.g. a product of two single-qubit states), single-qubit operations are performed using small-amplitude pulses that are resonant with individual qubits. These pulses are typically weak enough that the single-qubit operations are performed over times that are long compared to  $1/|\Delta_1 - \Delta_2|$  (the energy difference  $|\Delta_1 - \Delta_2|$  is used here because it is, to a good approximation, the smallest energy difference in the spectrum of the four lowest energy levels). Rather than perform ideal single-qubit operations, such weak pulses drive transitions between the eigenstates of the Hamiltonian of the entire system, regardless of the form of these eigenstates. One could therefore ignore the fact that  $|\psi_{nm}\rangle \neq |nm\rangle$  and simply use the eigenstates of the Hamiltonian (i.e.  $|\psi_{00}\rangle$ ,  $|\psi_{01}\rangle$ ,  $|\psi_{10}\rangle$  and  $|\psi_{11}\rangle$ ) as the computational basis for performing a quantum algorithm. One can then use weak pulses with properly calibrated frequencies to perform any operation on this effective two-qubit system. Thus the initial and all subsequent states in the experiment can be very close to the desired form, except that the computational basis does not have the simple, separable form [e.g., the state  $(|\psi_{00}\rangle + |\psi_{10}\rangle)/\sqrt{2}$  is prepared instead of the state  $(|00\rangle + |10\rangle)/\sqrt{2}$ ].

There are two main possible sources of errors that can affect the above picture. They are both related to the fact that in most quantum algorithms one needs to perform operations on a certain qubit without knowing the states of the other qubits. The residual-coupling Hamiltonian (Eq. 25) provides the first source of errors. The resonance frequencies for the transitions  $|\psi_{00}\rangle \leftrightarrow |\psi_{10}\rangle$  and  $|\psi_{01}\rangle \leftrightarrow |\psi_{11}\rangle$  are shifted from each other by a frequency difference given by  $4J_{\text{residual}}$ . As a result, the resonance frequency for performing operations on qubit 1 depends on the state of qubit 2, and vice versa. In principle, one could perform a single-qubit gate using two pulses, with each pulse being resonant with one of the transitions. This approach, however, is impractical for many-qubit systems, where resonance lines generally split into an exponentially large number of lines. A more scalable alternative is to perform single-qubit operations

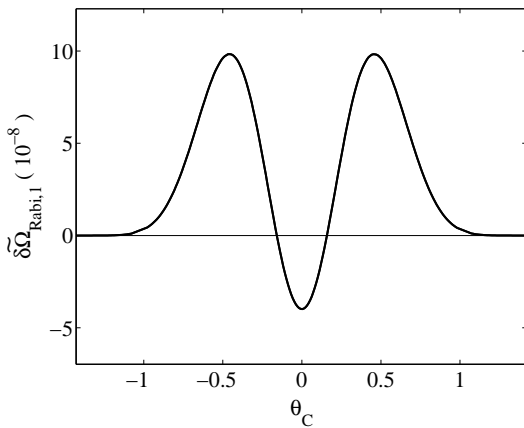


FIG. 3: The error-estimating quantity  $\widetilde{\delta\Omega}_{\text{Rabi},1} \equiv (\langle\psi_{00}|\hat{\sigma}_x^{(1)}|\psi_{10}\rangle - \langle\psi_{01}|\hat{\sigma}_x^{(1)}|\psi_{11}\rangle)/2$  for the relative spread in the Rabi frequency of qubit 1 as a function of the coupler's bias point  $\theta_C$  for the same parameters as in Fig. 2. Similar results would be obtained for qubit 2.

using driving amplitudes that are large compared to the spread in the relevant resonance frequencies, such that the pulse can be considered on resonance for all the relevant transitions. However, the residual-coupling Hamiltonian will still cause an undesirable phase accumulation over the course of running the algorithm. Until this residual coupling is suppressed in future experiments, one might need to apply refocussing pulses to reduce its effects. As can be seen from Figs. 1 and 2, pushing  $J_{\text{residual}}$  to the kHz range is possible using realistic experimental parameters. The other possible source of errors is the fact that the Rabi frequency of qubit 1 oscillations generally depends on the state of qubit 2, and vice versa. Such errors can be described by quantities of the form  $\widetilde{\delta\Omega}_{\text{Rabi},1} \equiv (\langle\psi_{10}|\hat{\sigma}_x^{(1)}|\psi_{00}\rangle - \langle\psi_{11}|\hat{\sigma}_x^{(1)}|\psi_{01}\rangle)/2$ . It is straightforward to see that, to the lowest order given in Sec. IV.C,

$$\langle\psi_{10}|\hat{\sigma}_x^{(1)}|\psi_{00}\rangle = \langle\psi_{11}|\hat{\sigma}_x^{(1)}|\psi_{01}\rangle. \quad (36)$$

In order to obtain an estimate for  $\widetilde{\delta\Omega}_{\text{Rabi},1}$ , we perform some numerical calculations. We show in Fig. 3 the results for the parameters of Fig. 2. We can see that  $\widetilde{\delta\Omega}_{\text{Rabi},1} \sim 10^{-8}$ . This type of errors can therefore be made extremely small using realistic experimental parameters.

Two more points of potential concern should be mentioned. The first relates to quantities of the form  $\langle\psi_{00}|\hat{\sigma}_x^{(1)}|\psi_{01}\rangle$ . This quantity describes, in some sense, how much qubit 2 “feels” a signal applied to qubit 1. Using the parameters of Fig. 2, this error estimator is of order  $10^{-2}$ , and vanishes close to the point where  $J = 0$ . This type of errors can be suppressed further by using microwave amplitudes such that the small fraction of the signal that is felt by qubit 2 is small enough to be considered far off resonance. Alternatively, one could say that single-qubit operations on qubit 1 must be performed on

a time scale long compared to  $|\langle\psi_{00}|\hat{\sigma}_x^{(1)}|\psi_{01}\rangle|/|\Delta_1 - \Delta_2|$ . This is a very mild constraint, even for existing experiments.

Finally, a tricky issue related to the usual theoretical approach mentioned at the beginning of this subsection is when the coupler degrees of freedom are traced out at the end of the actual quantum calculation. Here again, the measurement process in typical experiments does not follow the simple picture of a sudden, accurate measurement device that probes the basis 0/1. For flux qubits, for example, one typically measures the flux generated by the qubits and going through the loop of a readout SQUID. In principle, the readout device is simply a very accurate device for measuring magnetic fields. If the qubit-SQUID coupling is weak compared to the qubits' energy scale, the readout device will perform the measurement in the basis of the eigenstates of the system Hamiltonian, not the physically defined clockwise and counterclockwise current states [40]. We therefore find that the readout device can, in principle, give the correct reading (0 or 1) essentially 100% of the time even if the eigenstates that are being used in the experiment contain finite amplitudes of the ‘wrong’ state.

## B. Multi-qubit systems

In order to clearly identify whether a given effects is related to mediated coupling or not, we start by considering a multi-qubit system with no couplers (The expressions obtained below for the errors also apply if we integrate out the couplers in the circuit and use the effective, i.e. direct-plus-mediated, coupling strengths between the qubits). We first take the two-qubit Hamiltonian:

$$\hat{H} = \frac{\Delta_1}{2}\hat{\sigma}_z^{(1)} + \frac{\Delta_1}{2}\hat{\sigma}_z^{(2)} + J_{12}\hat{\sigma}_x^{(1)} \otimes \hat{\sigma}_x^{(2)}. \quad (37)$$

The above Hamiltonian has the interesting property that, with the proper assignment of the labels 00, 01, 10 and 11 to the eigenstates of the Hamiltonian, the relations

$$\begin{aligned} E_{10} - E_{00} &= E_{11} - E_{01} \\ E_{01} - E_{00} &= E_{11} - E_{10} \\ \langle\psi_{10}|\hat{\sigma}_x^{(1)}|\psi_{00}\rangle &= \langle\psi_{11}|\hat{\sigma}_x^{(1)}|\psi_{01}\rangle \\ \langle\psi_{01}|\hat{\sigma}_x^{(1)}|\psi_{00}\rangle &= \langle\psi_{11}|\hat{\sigma}_x^{(2)}|\psi_{10}\rangle \end{aligned} \quad (38)$$

hold regardless of the values of the different parameters in the Hamiltonian. The above relations imply that the first two sources of error discussed in the previous subsection vanish completely for this system. It is therefore not required to have  $J_{12} < |\Delta_1 - \Delta_2|$  in order to perform an almost error-free quantum algorithm in this system.

The question now is whether this situation persists for a system with more than two qubits. We approach this question by performing numerical simulations of a one-dimensional chain of three to ten qubits with the Hamil-

tonian:

$$\hat{H} = \sum_{j=1}^N \frac{\Delta_j}{2} \hat{\sigma}_z^{(j)} + \sum_{j=1}^{N-1} J_{j,j+1} \hat{\sigma}_x^{(j)} \otimes \hat{\sigma}_x^{(j+1)}. \quad (39)$$

From the numerical calculations we find that the generalized version of the relations in Eq. (38) holds only for the two qubits at the ends of the chain. The generalized version of the transition-frequency relation [i.e. the first two lines in Eq. (38)] continues to hold for all the qubits (i.e. the transition frequency for flipping qubit  $j$  is independent of the states of all the other qubits). The Rabi frequency of qubit  $j$  oscillations, however, now generally depends on the states of the other qubits. It is for this reason that one would like to set  $J = 0$  in the off state, even though violating this requirement does not necessarily have detrimental effects on a two-qubit experiment.

In order to get an estimate for the above-mentioned errors, we take the three-qubit case and calculate the standard deviation  $\widetilde{\delta\Omega}_{\text{Rabi},2}$  in the quantity  $\langle \psi_{n1m} | \hat{\sigma}_x^{(2)} | \psi_{n0m} \rangle$ . When the coupling strengths  $J_{j,j+1}$  are small compared to the differences between qubit gaps, we find that

$$\widetilde{\delta\Omega}_{\text{Rabi},2} \approx 1.2 \frac{J_{12}^2 J_{23}^2}{|(\Delta_1 - \Delta_2)(\Delta_2 - \Delta_3)(\Delta_1 - \Delta_3)^2|}. \quad (40)$$

It will therefore be highly desirable in future experiments to set the coupling strengths (to leading order) between all neighbouring qubits to zero. It will also be highly desirable to set the gaps  $\Delta_j$  to different values, even if they are not nearest neighbours.

We now take a three-qubit chain with couplers, and we perform numerical simulations for several sets of parameters with the leading-order coupling strengths (i.e. the parameters that correspond to  $J$  in the two-qubit case) set to zero. We calculate the transition frequencies for qubit  $j$  ( $j = 1, 2, 3$ ) for the four different states of the two other qubits. We find that the frequency shifts are consistent with the residual coupling strength given in Eq. (29). We therefore expect our results concerning the residual coupling to hold for systems with more than two qubits. We also expect the form of the eigenstates to follow the rather straightforward generalization of Eq. (31). If a distant pair of qubits have the same value of  $\Delta_j$ , the energy scale associated with any possible hybridization of energy levels (e.g. involving states of the form  $|00n_20n_30n_4010n_6\dots\rangle$  and  $|10n_20n_30n_4000n_6\dots\rangle$ ) will be small enough that it can be neglected. Similarly, hybridization between energy levels that require flipping the states of several qubits should be greatly suppressed.

Finally, we consider a loop of three or four qubits, i.e. in triangle and square geometries. Denoting the typical scale of the coupling strengths between neighbouring qubits by  $J$  and the detuning between qubits by  $\Delta\omega$ , which is taken to be much smaller than the qubit frequencies, we find that the standard deviation in the resonance frequency  $\delta\omega_{\text{resonance}}$  and the standard deviation

in the transition matrix element  $\widetilde{\delta\Omega}_{\text{Rabi}}$  when attempting to change the state of a given qubit are given by

$$\begin{aligned} \delta\omega_{\text{resonance}} &\sim \frac{J^3}{\Delta\omega^2} \\ \widetilde{\delta\Omega}_{\text{Rabi}} &\sim \left(\frac{J}{\Delta\omega}\right)^3 \end{aligned} \quad (41)$$

in the three qubit case and

$$\delta\omega_{\text{resonance}} \sim \frac{J^4}{\Delta\omega^3} \quad (42)$$

$$\widetilde{\delta\Omega}_{\text{Rabi}} \sim \left(\frac{J}{\Delta\omega}\right)^4 \quad (43)$$

in the four qubit case. The detailed expressions for the above quantities depend rather nontrivially on the values of the different parameters in the problem. Errors stemming from these spreads in resonance and Rabi frequencies therefore depend on the geometry of the multi-qubit system, i.e. chain versus closed loop. A two-dimensional lattice would belong to the latter category.

## VI. CONCLUSION

We have analyzed the problem of a high-excitation-energy quantum object mediating coupling between two qubits. After reviewing some known results concerning the leading-order term in the mediated coupling, we obtained expressions for the residual-coupling Hamiltonian in the off state and the entanglement in the eigenstates of the system. We have argued that our approach analyzing the eigenstates of the entire system is the appropriate one to describe recent, and possibly future, experiments. We have also estimated the expected errors originating from the non-ideality of the off state in typical experimental situations. Our results should be helpful in designing future circuits that employ a high-excitation-energy coupler to achieve tunable coupling between qubits. In particular, our results suggest that with properly chosen design parameters, the residual coupling in the off state could be greatly reduced in future experiments.

We have focused on the case of a two-qubit system, which is the relevant case for present-day experiments. However, we expect our results for the errors in a two-qubit system to apply to multi-qubit systems as well. We have also shown that other sources of error that are absent in a two-qubit system arise for systems with more than two qubits. It would therefore be interesting and important in the future to analyze in more detail the properties of large, many-qubit systems.

### Appendix: Quasi-degenerate perturbation theory

In this appendix we present a perturbation-theory procedure for the case where the separation between some

energy levels is not large compared to the energy scale of the perturbation [34].

Let us take the Hamiltonian

$$\hat{H} = \hat{H}_0 + \hat{V}, \quad (44)$$

where we want to treat  $\hat{V}$  as a perturbation. We assume, however, that the energy scale of  $\hat{V}$  is not necessarily small compared to the energy separations within a subset of  $n$  eigenstates of  $\hat{H}_0$ . The energy scale of  $\hat{V}$  is small compared to the energy separation between this subset of levels and all the levels outside it.

We now want to find the approximate energy levels and eigenstates of  $\hat{H}$  in the vicinity of these  $n$  original energy levels of  $\hat{H}_0$ . We proceed by assuming that these closely spaced eigenstates can have a large amount of mixing among themselves because of the added perturbation  $\hat{V}$ ,

but we assume that mixing with all other states will be small. In other words, we express (any one of) the eigenstates of interest as:

$$|\Psi_i\rangle = \sum_{j=1}^n f_{ij} |\psi_j\rangle + \sum_{j=n+1}^{\infty} g_{ij} |\psi_j\rangle \quad (45)$$

where  $|\psi_j\rangle$  are the eigenstates of  $\hat{H}_0$  with

$$\hat{H}_0 |\psi_j\rangle = \epsilon_j |\psi_j\rangle, \quad (46)$$

the states  $|\Psi_i\rangle$  with  $j = 1, 2, \dots, n$  represent the states of interest, and  $g_{ij}$  are understood to be small enough to be treated perturbatively (this is the only reason we express the amplitudes  $f_{ij}$  and  $g_{ij}$  using two different symbols). We can now express the eigenvalue problem as:

---


$$\sum_{j=1}^n f_{ij} \epsilon_j |\psi_j\rangle + \sum_{j=n+1}^{\infty} g_{ij} \epsilon_j |\psi_j\rangle + \sum_{k=1}^{\infty} \left( \sum_{j=1}^n f_{ij} V_{kj} |\psi_k\rangle + \sum_{j=n+1}^{\infty} g_{ij} V_{kj} |\psi_k\rangle \right) = E_i \left( \sum_{j=1}^n f_{ij} |\psi_j\rangle + \sum_{j=n+1}^{\infty} g_{ij} |\psi_j\rangle \right). \quad (47)$$


---

If we multiply the above equation from the left by  $\langle \psi_l |$  with  $1 \leq l \leq n$ , we obtain the equation:

$$f_{il} \epsilon_l + \sum_{j=1}^n f_{ij} V_{lj} + \sum_{j=n+1}^{\infty} g_{ij} V_{lj} = E_i f_{il}. \quad (48)$$

If we multiply the equation by  $\langle \psi_l |$  with  $l > n$ , we obtain instead:

$$g_{il} \epsilon_l + \sum_{j=1}^n f_{ij} V_{lj} + \sum_{j=n+1}^{\infty} g_{ij} V_{lj} = E_i g_{il} \quad (49)$$

Equation (49) is now treated using a perturbative (or iterative) approach. If we neglect the sum over the states with  $j = n + 1, \dots$ , we obtain:

$$g_{il} \approx \frac{\sum_{j=1}^n f_{ij} V_{lj}}{E_i - \epsilon_l}. \quad (50)$$


---

Substituting this expression into Eq. (48), we obtain:

$$\sum_{j=1}^n \left( \epsilon_l \delta_{lj} + V_{lj} + \sum_{j'=n+1}^{\infty} \frac{V_{lj'} V_{j'j}}{E_i - \epsilon_{j'}} \right) f_{ij} = E_i f_{il}, \quad (51)$$

where  $\delta_{lj}$  is the Kronecker delta function.

If we want to obtain more accurate results, we can take Eq. (50) and substitute it into the left-hand side of Eq. (49). Expressing  $g_{ij}$  in Eq. (50) as  $g_{ij}^{\text{prev}}$ , we obtain:

$$\begin{aligned} g_{il} &\approx \frac{\sum_{j=1}^n f_{ij} V_{lj}}{E_i - \epsilon_l} + \frac{1}{E_i - \epsilon_l} \left( \sum_{j=n+1}^{\infty} g_{ij}^{\text{prev}} V_{lj} \right) \\ &= \frac{\sum_{j=1}^n f_{ij} V_{lj}}{E_i - \epsilon_l} + \frac{1}{E_i - \epsilon_l} \left( \sum_{j=n+1}^{\infty} \frac{\sum_{j'=1}^n f_{ij'} V_{jj'}}{E_i - \epsilon_j} V_{lj} \right). \end{aligned} \quad (52)$$

Using this expression for  $g_{ij}$  in Eq. (48), we find that to the next order:

$$\sum_{j=1}^n \left( \epsilon_l \delta_{lj} + V_{lj} + \sum_{j'=n+1}^{\infty} \frac{V_{lj'} V_{j'j}}{E_i - \epsilon_{j'}} + \sum_{j'=n+1}^{\infty} \sum_{j''=n+1}^{\infty} \frac{V_{lj'} V_{j'j''} V_{j''j}}{(E_i - \epsilon_{j'})(E_i - \epsilon_{j''})} \right) f_{ij} = E_i f_{ij}. \quad (53)$$

The generalization to all orders is now obvious, if needed. One must be careful, of course, that the denominators on the left-hand side of Eqs. (51) and (53) contain the eigenvalue  $E_i$ . The solution is therefore not yet obtained by a straightforward diagonalization of an  $n \times n$  matrix. However, it is usually a good first approximation to use some (averaged) value for  $E_i$  in the denominator. This value can be taken from the energy levels of the original Hamiltonian  $\hat{H}_0$ . One can then obtain more accurate results by introducing a second iterative procedure. Every time we obtain an approximate value of the energy  $E_i$ , we can substitute it into the left-hand side of Eq. (51) or (53) to obtain an even more accurate result.

## ACKNOWLEDGMENTS

We would like to thank M. Grajcar, J. R. Johansson, A. Maassen van den Brink and J. Q. You for useful discussions. This work was supported in part by the National Security Agency (NSA), the Army Research Office (ARO), the Laboratory for Physical Sciences (LPS), the National Science Foundation (NSF) grant No. EIA-0130383 and the Japan Society for the Promotion of Science Core-To-Core (JSPS CTC) program. One of us (S.A.) was supported by the Japan Society for the Promotion of Science (JSPS).

- 
- [1] For recent reviews on the subject, see e.g. J. Q. You and F. Nori, *Phys. Today* **58** (11), 42 (2005); G. Wendin and V. Shumeiko, in *Handbook of Theoretical and Computational Nanotechnology*, ed. M. Rieth and W. Schommers (ASP, Los Angeles, 2006).
  - [2] Yu. A. Pashkin, T. Yamamoto, O. Astafiev, Y. Nakamura, D. V. Averin and J. S. Tsai, *Nature* **421**, 823 (2003).
  - [3] P. R. Johnson, F. W. Strauch, A. J. Dragt, R. C. Ramos, C. J. Lobb, J. R. Anderson, and F. C. Wellstood, *Phys. Rev. B* **67**, 020509(R) (2003).
  - [4] A. J. Berkley, H. Xu, R. C. Ramos, M. A. Gubrud, F. W. Strauch, P. R. Johnson, J. R. Anderson, A. J. Dragt, C. J. Lobb, and F. C. Wellstood, *Science* **300**, 1548 (2003).
  - [5] T. Yamamoto, Yu. A. Pashkin, O. Astafiev, Y. Nakamura, and J. S. Tsai, *Nature* **425**, 941 (2003).
  - [6] A. Izmalkov, M. Grajcar, E. Il'ichev, Th. Wagner, H.-G. Meyer, A. Yu. Smirnov, M. H. S. Amin, A. Maassen van den Brink, and A. M. Zagoskin, *Phys. Rev. Lett.* **93**, 037003 (2004).
  - [7] H. Xu, F. W. Strauch, S. K. Dutta, P. R. Johnson, R. C. Ramos, A. J. Berkley, H. Paik, J. R. Anderson, A. J. Dragt, C. J. Lobb, and F. C. Wellstood, *Phys. Rev. Lett.* **94**, 027003 (2005).
  - [8] R. McDermott, R. W. Simmonds, M. Steffen, K. B. Cooper, K. Cicak, K. D. Osborn, S. Oh, D. P. Pappas, and J. Martinis, *Science* **307**, 1299 (2005).
  - [9] J. B. Majer, F. G. Paauw, A. C. J. ter Haar, C. J. P. M. Harmans, and J. E. Mooij, *Phys. Rev. Lett.* **94**, 090501 (2005).
  - [10] B. L. T. Plourde, T. L. Robertson, P. A. Reichardt, T. Hime, S. Linzen, C.-E. Wu, and J. Clarke, *Phys. Rev. B* **72**, 060506(R) (2005).
  - [11] M. Grajcar, A. Izmalkov, S. H. W. van der Ploeg, S. Linzen, T. Plecenik, Th. Wagner, U. Hübner, E. Il'ichev, H.-G. Meyer, A. Yu. Smirnov, P. J. Love, A. Maassen van den Brink, M. H. S. Amin, S. Uchaikin, and A. M. Zagoskin, *Phys. Rev. Lett.* **96**, 047006 (2006).
  - [12] M. Steffen, M. Ansmann, R. C. Bialczak, N. Katz, E. Lucero, R. McDermott, M. Neeley, E. M. Weig, A. N. Cleland, J. M. Martinis, *Science*, **313**, 1423 (2006).
  - [13] S. H. W. van der Ploeg, A. Izmalkov, A. Maassen van den Brink, U. Huebner, M. Grajcar, E. Il'ichev, H.-G. Meyer, A. M. Zagoskin, *Phys. Rev. Lett.* **98**, 057004 (2007).
  - [14] R. Harris, A. J. Berkley, M. W. Johnson, P. Bunyk, S. Govorkov, M. C. Thom, S. Uchaikin, A. B. Wilson, J. Chung, E. Holtham, J. D. Biamonte, A. Yu. Smirnov, M. H. S. Amin, A. Maassen van den Brink, *Phys. Rev. Lett.* **98**, 177001 (2007).
  - [15] T. Hime, P. A. Reichardt, B. L. T. Plourde, T. L. Robertson, C.-E. Wu, A. V. Ustinov, and J. Clarke, *Science* **314**, 1427 (2006).
  - [16] A. O. Niskanen, K. Harrabi, F. Yoshihara, Y. Nakamura, J. S. Tsai, *Phys. Rev. B* **74**, 220503 (2006).
  - [17] A. O. Niskanen, K. Harrabi, F. Yoshihara, Y. Nakamura, S. Lloyd, J. S. Tsai, *Science* **316**, 723 (2007).
  - [18] J. Plantenberg, P. C. de Groot, C. J. P. M. Harmans and J. E. Mooij, *Nature* **447**, 836 (2007).
  - [19] J. B. Majer *et al.*, unpublished.
  - [20] D. V. Averin and C. Bruder, *Phys. Rev. Lett.* **91**, 057003 (2003).
  - [21] B. L. T. Plourde, J. Zhang, K. B. Whaley, F. K. Wilhelm, T. L. Robertson, T. Hime, S. Linzen, P. A. Reichardt, C.-E. Wu, and J. Clarke *Phys. Rev. B* **70**, 140501(R) (2004).
  - [22] M. Wallquist, J. Lantz, V. S. Shumeiko, and G. Wendin, *New J. Phys.* **7**, 178 (2005)
  - [23] A. Maassen van den Brink, A. J. Berkley, M. Yalowsky, *New J. Phys.* **7**, 230 (2005).
  - [24] Before Refs. [20, 21, 23] there had been proposals to couple superconducting charge qubits using a large inductance; see, e.g., A. Shnirman, G. Schön, and Z. Hermon, *Phys. Rev. Lett.* **79**, 2371 (1997); Y. Makhlin, G. Schön, and A. Shnirman, *Nature* **398**, 305 (1999). Smaller inductances were considered in J. Q. You, J. S. Tsai, and

- F. Nori, Phys. Rev. Lett. **89**, 197902 (2002). A similar approach for flux qubits was proposed in J. Q. You, Y. Nakamura, and F. Nori, Phys. Rev. B **71**, 024532 (2005).
- [25] E. Farhi and S. Gutmann, Phys. Rev. A **57**, 2403 (1998); E. Farhi, J. Goldstone, S. Gutmann, and M. Spiser, quant-ph/0001106.
- [26] P. Bertet, C. J. P. M. Harmans, and J. E. Mooij, Phys. Rev. B **73**, 064512 (2006).
- [27] A. O. Niskanen, Y. Nakamura, and J. S. Tsai, Phys. Rev. B **73**, 094506 (2006).
- [28] M. Grajcar, Y.-X. Liu, L.-F. Wei, and F. Nori, Phys. Rev. B **74**, 172505 (2006).
- [29] Performing two-qubit gates on superconducting qubits by driving the qubits at the sum or difference of their characteristic frequencies was first proposed in Y.-X. Liu, L.-F. Wei, J. S. Tsai, and F. Nori, Phys. Rev. Lett. **96**, 067003 (2006).
- [30] There are a large number of theoretical studies on this subject. See, e.g., J. Q. You and F. Nori, Phys. Rev. B **68**, 064509 (2003); R. Migliore, A. Konstadopoulou, A. Vourdas, T. P. Spiller, and A. Messina, Phys. Lett. A **319**, 67 (2003); Y.-X. Liu, L. F. Wei, J. S. Tsai, and F. Nori, arXiv:cond-mat/0509236; A. Blais, J. Gambetta, A. Wallraff, D. I. Schuster, S. M. Girvin, M. H. Devoret, and R. J. Schoelkopf, Phys. Rev. A **75**, 032329 (2007); H. Nakano, K. Kakuyanagi, M. Ueda, and K. Semba, Appl. Phys. Lett. **91**, 032501 (2007); F. Helmer, M. Mariantoni, A. G. Fowler, J. von Delft, E. Solano, F. Marquardt, arXiv:0706.3625.
- [31] C. Hutter, A. Shnirman, Y. Makhlin, and G. Schön, Europhys. Lett. **74**, 1088 (2006).
- [32] A. Maassen van den Brink, J. R. Johansson, and F. Nori, unpublished.
- [33] See, e.g., G. Baym, *Lectures on Quantum Mechanics* (Addison-Wesley, New York, 1990).
- [34] See, e.g., J. J. Sakurai, *Modern Quantum Mechanics* (Addison-Wesley, New York, 1994).
- [35] In the theoretical treatment of this system, one can also rewrite the Hamiltonian such that the matrix elements  $A_{00}$  and  $B_{00}$  are absorbed into  $\epsilon_1$  and  $\epsilon_2$ . One then replaces  $A_{ll}$  by  $A_{ll} - A_{00}$ , and similarly for  $\hat{B}$ .
- [36] Note that the reason why the results come with the operators  $\hat{\sigma}_z^{(j)}$  is the fact that the preferred basis, determined from the lowest-order calculation, is diagonal in  $\hat{\sigma}_z^{(1)}$  and  $\hat{\sigma}_z^{(2)}$ .
- [37] The second term on the right-hand side of Eq. (31) is obtained by including the gaps  $\Delta_j$  in the denominator in Eq. (51), which slightly modifies  $J_1$  depending on the eigenstate under consideration.
- [38] M. Wallquist, V. S. Shumeiko, G. Wendin, Phys. Rev. B **74**, 224506 (2006). Note that, strictly speaking, the coupler is no longer an harmonic, i.e. linear, oscillator in this design.
- [39] See, e.g., C. Rigetti, A. Blais, and M. Devoret, Phys. Rev. Lett. **94**, 240502 (2005); G. S. Paroanu, Phys. Rev. B **74**, 140504(R) (2006); S. Ashhab, S. Matsuo, N. Hatakenaka, and F. Nori, Phys. Rev. B **74**, 184504 (2006); See also Ref. [29].
- [40] For example, it is possible, in principle, for a device that couples to the operator  $\hat{\sigma}_z$  of a two-level system to distinguish with essentially 100% fidelity between eigenstates of the form  $\sqrt{0.6}|0\rangle + \sqrt{0.4}|1\rangle$  and  $\sqrt{0.4}|0\rangle - \sqrt{0.6}|1\rangle$ .